Microchimica Acta (2019) 186:574
https://doi.org/10.1007/s00604-019-3689-x

ORIGINAL PAPER

Fluorometric determination of microRNA by using an entropy-driven three-dimensional DNA walking machine based on a catalytic hairpin assembly reaction on polystyrene microspheres

Tingyan Yang[1] · Jie Fang[1] · Yongcan Guo[2] · Shangchun Sheng[3] · Qinli Pu[1] · Li Zhang[1] · Xinying Ou[1] · Ling Dai[1] · Guoming Xie[1]

Received: 10 April 2019 / Accepted: 7 July 2019

Abstract

An entropy-driven 3-D DNA walking machine is presented which involves catalytic hairpin assembly (CHA) for detection of microRNA. A 3-D DNA walking machine was designed that uses streptavidin-coated polystyrene microspheres as track carriers to obtain reproducibility. The method was applied to microRNA 21 as a model analyte. Continuous walking on the DNA tracks is achieved via entropy increase. This results in a disassembly of ternary DNA substrates on polystyrene microspheres and leads to cycling of microRNA 21. The release of massive auxiliary strands from ternary DNA substrates induces the CHA. This is accompanied by in increase in fluorescence, best measured at excitation/emission wavelengths of 480/520 nm. On account of entropy-driven reaction, the assay is remarkably selective. It can differentiate microRNA 21 from homologous microRNAs in giving a signal that is less than 5% of the signal for microRNA 21 except for microRNA-200b. The assay works in the 50 pM to 20 nM concentration range and has a 41 pM detection limit. The method displays good reproducibility (between 1.1 and 4.2%) and recovery (from 99.8 to 104.0%).

Keywords Enzyme-free assay · Fluorescent biosensor · Toehold-mediated strand displacement reaction · DNA machines · Nucleic acid assay

Introduction

DNA machines are molecular machines constructed by DNA, which can be logically designed since the versatility and predictability of well-defined Watson–Crick base pairing rule [1, 2]. Various DNA machines have been constructed and synthesized by highly programmable approaches, such as DNA tweezers [3], DNA motors [4], DNA walkers [5] and DNA robots [6]. Among them, DNA walking machines can be controlled accurately in the programmed oligonucleotide tracks on the microscale or nanoscale and possess significant application potential in biosensors [7–9], biocomputing [10] and drug-delivery [11]. Previous studies have reported engineered DNA walking machines moving along the designed tracks on one-dimensional (1D) footpaths [12, 13], two-dimensional (2D) origami [14, 15], or three-dimensional (3D) landscapes [16, 17]. In particular, 3-D DNA tracks possess more powerful amplification capability. This is ascribed to that all reaction components are conjugated on microparticles or nanoparticles, resulting in high local effective concentration and stable signal outputs [18–20]. Therefore, the application of 3-D DNA walking machines has already attracted close attention. For example, Li and co-workers designed an enzyme-powered DNA walker sensor with 3-D track that was

Electronic supplementary material The online version of this article (https://doi.org/10.1007/s00604-019-3689-x) contains supplementary material, which is available to authorized users.

✉ Guoming Xie
guomingxie@cqmu.edu.cn; xiegm059@foxmail.com

[1] Key Laboratory of Laboratory Medical Diagnostics of Education, Ministry of Education, Department of Laboratory Medicine, Chongqing Medical University, No. 1 Yi Xue Yuan Road, Chongqing 400016, People's Republic of China

[2] Clinical Laboratory of Traditional Chinese Medicine Hospital Affiliated to Southwest Medical University, Luzhou 646000, People's Republic of China

[3] Clinical Laboratory of Hospital Affiliated to Chengdu University, Chengdu 610081, People's Republic of China

Published online: 24 July 2019

able to achieve isothermal and homogeneous signal amplification for specific nucleic acids detection [21]. Fan et al. engineered an exonuclease III-powered stochastic DNA walker, which can lead to cascade signal amplification for ultrasensitive bioanalysis [22]. Liu and co-workers described a 3-D DNA walker for determination of 8-hydroxy-2′-deoxyguanosine that was three orders of magnitude lower compared to previously reported methods [23]. Although these methods have exhibited high sensitivity, they are enzyme-dependent with the disadvantages of being vulnerable to complex experiment conditions (e.g. buffer and temperature), high detection costs, and bad long-term storage [24]. Accordingly, the research of non-enzymatic 3-D DNA walking machines has received desirable attention.

Previously, Ye and co-workers reported a rational engineered DNA walker with 3-D tracks on AuNPs by entropy-driven reaction (EDR) [25]. In contrast to enzyme-depended signal amplification system, entropy-driven reaction is a catalytically signal amplification strategy without enzyme or precise temperature cycling. It is driven forward by entropy increase and applies a string of single nucleic acid strand to play multiple roles in the catalytic circuit via toehold-mediated strand displacement reaction [26]. Benefiting from its unique and extraordinary driving force, the total number of base pairs of the system retains invariant during the amplification process. Thus, this strategy offers fewer chances for circuit leakage and providing a more reliable platform for accurate detection [27]. With the assistance of EDR, the aforementioned 3-D DNA walking machine has superior sensitivity for microRNA imaging. Nevertheless, it used gold nanoparticles (AuNPs) as 3-D track carriers have inevitable limitations. On the one hand, DNA attachment to AuNPs is often performed via a thiol label. Such adsorption force is not strong enough and hard to avoid unintended DNA base adsorption, which hinders DNA hybridization reducing colloidal stability [28]. On the other hand, it requires immobilization of affinity ligand and ternary DNA substrates on the surface of AuNPs and optimization of each concomitantly, which results in poor reproducibility of the conjugate.

One plausible way to deal with above-mentioned troubles rest on the exploration of other substrate carriers for DNA immobilization. Due to the large surface area and high surface reaction capability, monodisperse polystyrene microspheres are widely applied in DNA barcode for detection [29, 30]. More importantly, commercialized streptavidin-coated polystyrene microspheres can be easily functionalized through streptavidin-biotin conjugation and with promising reproducibility. The conjugation between streptavidin and biotin is much more stronger than Au-S bond. Therefore, streptavidin-coated polystyrene microspheres can serve as potential substrate carriers to construct 3-D DNA walking machines. In the meantime, isothermal amplification strategy has attracted increasing interest for constructing DNA machines for the sensitive detection of biomolecules [31]. Catalytic hairpin assembly (CHA) is a cost-effective and enzyme-free cascade amplification strategy [32–35]. The advantages of both entropy-driven 3D-DNA walking machines and CHA have attracted our interest in the field of nucleic acid detection.

An entropy-driven 3-D DNA walking machine which involves CHA cascade amplification was constructed to realize sensitive detection of picomolar level of microRNA. We use microRNA 21 as a model target that is closely related to a lot of disease include cancer in blood. In this system, microRNA 21 acts as a catalyzer and stochastic DNA walker, which moves continually over microspheres surface. This leads to continuous disassembly of ternary DNA substrates and release a large number of auxiliary strand (AS) to realize cycle of microRNA 21. In addition, AS can catalyze CHA reaction for producing high signal output. The entropy-driven reaction has high specificity because it can clearly distinguish the change of one base. We anticipate that this sensor would provide a potential platform for microRNA analysis.

Experimental

Reagents and materials

All HPLC-purified oligonucleotide sequences used in this work were synthesized by Shanghai Sangon Biological Engineering Technology & Services Co. Ltd. (Shanghai, China, http://www.sangon.com). Streptavidin-coated polystyrene microspheres were purchased from Spherotech (http://www.spherotech.com). Agarose G-10 was supplied by Biowest, Inc. (Spain, http://www.biowest.net). A 20 bp DNA Ladder, loading buffer (6×) and Gel Red nucleic acid dye were obtained from TaKaRa Biotechnology Co. Ltd. (Dalian, China, http://www.takara.com cn). 5× Tris-borate-EDTA (TBE), 50 × Tris-acetate-EDTA (TAE), 1 M Tris•HCl buffer and DEPC H_2O were purchased from Shanghai Sangon Biological Engineering Technology& Services Co. Ltd. (Shanghai, China, http://www.sangon.com). Deionized (DI) water (Milli-Q 18.2 MΩ·cm, Millipore System Inc. (https://www.rephile.com/).) was employed in all runs. Cutsmart buffer was purchased from New England Biolabs. (the United States of America, https://www.neb.com/). TNaK buffer (20 mM Tris•HCl, pH 7.5; 140 mM NaCl; 5 mM KCl). Binding buffer (20 mM Tris•HCl, pH 7.5, 1 M NaCl, 1 mM EDTA, 0.0005% Triton X-100). and TEMg buffer: (10 mM Tris•HCl, 1 mM EDTA, 12.5 mM MgCl2, pH 8.0) were used as the reaction buffer. All other chemicals were of reagent grade and used as received.

Apparatus and measurements

All fluorescence signals were carried out on a Cary Eclipse Fluorescence Spectrophotometer (Agilent, California, http://www.agilent.com/) with quartz cuvette. Parameters: excitation wavelength, 480 nm; emission wavelength, 520 nm; excitation slit = 5 nm; emission slit = 10 nm. Electrophoresis apparatus DYY-6C (DYY6C, LiuYi, China, http://www.ly.com.cn/) was used in the electrophoresis experiment. Gel images were photographed by a UV digital imaging system (BioRad Laboratories, USA, http://www.bio-rad.com/). Parameters: voltage = 90 V, time = 60 min. Scanning electron microscope (SEM, SU8010, Hitachi, Japan) was employed to monitor the structures of streptavidin-coated polystyrene microspheres.

The fabrication of 3D DNA walking machine

Purified LS, AS, S and TEMg buffer were refolded to prepare LS/AS/S complex (C3) by annealing. The ratio of LS: AS: S is 1:1. 5:1.5. Annealing consisted of heating the solution to 95 °C for 5 min followed by slowly decreasing the temperature to 25 °C at a rate of 0.1 °C •second^{-1} in PCR instrument.

Streptavidin-coated polystyrene microspheres (PS, 50 μL) were washed two times with 50 μL binding buffer by centrifuging the particles at 12000 rpm for 5 min following by decanting the supernatant. After resuspension with 50 μL of binding buffer, 5 μL of 20 μM C3 was added into the 50 μL re-suspended PS. After incubation for 15 min at 37 °C, the complex was washed three times with 50 μL of TEMg buffer by centrifuging the microspheres at 12000 rpm for 5 min following by decanting the supernatant. Finally, C3/PS was prepared by resuspension with 50 μL of TEMg buffer.

Detection of microRNA by 3D DNA walking machine coupling CHA

Hairpin probe (H1), Hairpin probe2 (H2) were refolded by heating the solution to 95 °C for 5 min followed and slowly decreasing the temperature to 25 °C. An amount of 50 nM stock of RepF:RepQ complex was prepared by annealing 10 μM RepF and 20 μM RepQ in 1 × TNaK buffer.

For a typical 3D DNA walking machine operation, a reaction mixture containing 5 μL C3/PS, 2 μL of 10 μM fuel nucleic acid (FS), 33 μL cutsmart buffer, and 10 μL of the target with various concentrations was incubated at 37 °C for 60 min. After centrifuging, 40 μL of the supernatant was added to the mixture of 5 μL of 1 μM H1, 2 μL of 10 μM H2, 10 μL of 50 nM RepF: RepQ complex and 23 μL 1 × TNaK buffer, and reacted in the dark at 25 °C for 60 min to activate CHA reaction. Finally, fluorescence signals were measured using the spectrophotometer.

Gel electrophoresis

The 3.5% agarose gel was freshly prepared and agarose gel electrophoresis was carried out at a constant voltage at 90 V for 60 min. Different samples were added into lane 1: 20 bp DNA marker, lane 2: 1 μM C3, lane 3: 1 μM (C3 + F), lane 4: 1 μM (F + S), lane 5: 1 μM (C3 + F + microRNA21), lane 6: 2 μM microRNA21, lane 7: 2 μM F, lane 8: 2 μM S, lane 9: 1 μM (AS+H1 + H2), lane 10: 1 μM (H1 + H2), lane 11: 2 μM AS. The dye was GelRed™ nucleic acid gel stain. Electrophoresis apparatus (DYY-6C, LiuYi, China) was utilized for the electrophoresis experiments. Finally, the gels were recorded by Bio-Rad digital imaging system.

Results and discussion

Principle of the method

The schematic principle of this biosensor is depicted in Scheme. 1. Entropy-driven 3-D DNA walking machine consists of streptavidin-coated polystyrene microspheres and ternary DNA substrates which include linker strand (LS), auxiliary strand (AS), substrate strand (S). Sequences of the designed oligonucleotides are listed in the Supporting Information (**Table S1**) and all of the sequences used in this work were designed with Nupack (**Fig. S1** and **Fig. S2**). The 5′ terminal of link strand (LS) was labeled with biotin to immobilize ternary DNA substrates (C3) on streptavidin-coated polystyrene microspheres via streptavidin-biotin conjunction. The overall reaction started with the displacement of AS by microRNA21 (T) through the toehold domain 1 (in Scheme 1). This initiated the entropy-driven reactions and led to the release of the AS. Subsequently, another toehold domain 2 was exposed for hybridization with a fuel nucleic acid (F) to substitute and release T. The strand displacement reaction between the F and a substrate strand (SS) generated recycling of T (Cycle 1) and a waste strand (F/S). Furthermore, AS as an initiator to interact with free terminal of H1. Branch migration then opened hairpin H1 and formed AS/H1 intermediates. The newly generated toehold domain 3 (in Scheme 1) of H1 opened hairpin 2 (H2) to form H1:H2:AS complexes. Due to the instability of the complexes, AS was separated from it. This allows AS to serve as a catalyst to trigger the hybridization of additional pairs of H1 and H2 (Cycle 2). Two complementary oligonucleotide probes which consist of two strands, one labeled with FAM (RepF) at 5′ terminal and the other labeled with BHQ1 (RepQ) at 3′ terminal, were used as signal probes. Hybridization of these two oligonucleotide probes indeed result in efficient quenching of FAM. In the case of existing H1/H2 duplex, the free terminal of H1 in the H1/H2 duplex can hybridize with RepF through the

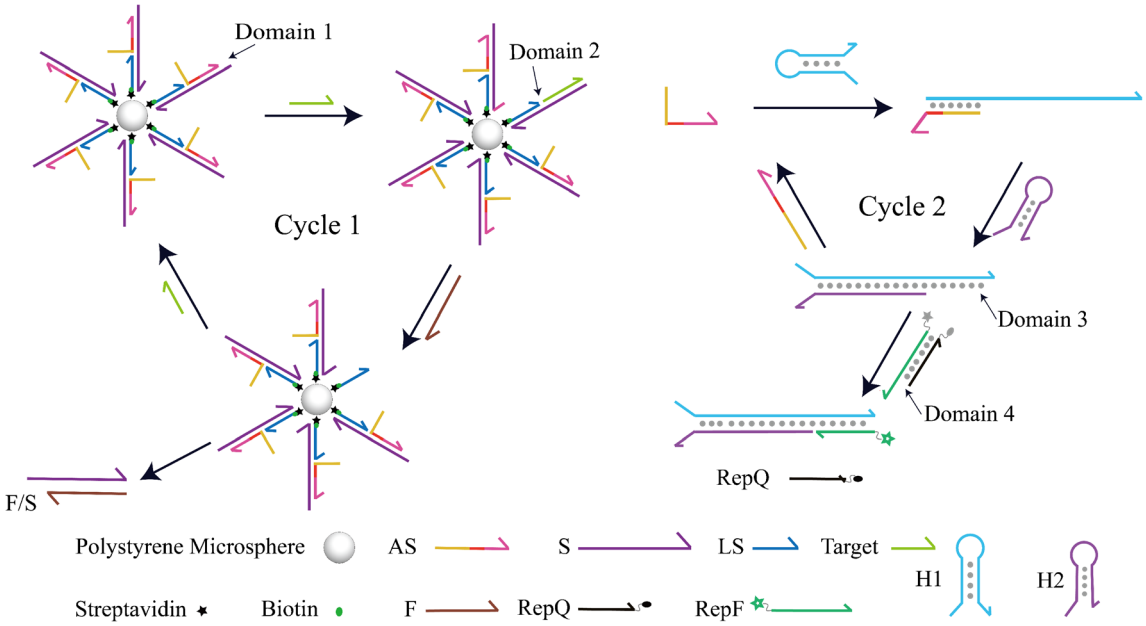

Scheme 1 Schematic presentation of the principle of the 3-D DNA walking machine combines with CHA

toehold domain 4. This resulted in increase in fluorescent signal of FAM.

Characterization of polystyrene microspheres

The scanning electron microscope (SEM) was used to characterize the streptavidin-coated polystyrene microspheres. **Fig. S3 a** and **b** show the SEM images of polystyrene microspheres at low and high magnification respectively. It can be observed that the polystyrene microspheres are highly uniform and well-dispersed. The average size is about 800 nm. The high quality of polystyrene microspheres insure the good performance of our 3-D DNA walking machine.

Feasibility of the method

The feasibility of the entropy-driven reaction was firstly verified. As displayed in Fig. 1a, the 5′ terminal of LS was labeled with biotin and the 3′ of S was labeled with FAM. In the presence of T and F, ternary DNA substrates were dissociated and a new band F/S was formed in solution. Then the fluorescence of the supernatant was detected by centrifugation (Fig. 1b, curve b). On the contrary, S will not be separated from the surface of polystyrene microspheres without target, and the supernatant will not have fluorescence (Fig. 1b, curve a). As depicted in Fig. 2, 3.5% agarose gel was used to testify the feasibility of EDR and CHA reaction separately. The slow mobility of C3 in Lane 2 clearly demonstrated the formation of ternary DNA substrates. Compared with lane 3 which was just in the presence of C3 and F, a new band F/S was observed and the lane of C3 was significantly disappeared in lane 5. Simultaneously, the bands of AS and H1/H2 complex were appeared in lane 9, which may be attributed to AS catalyzed CHA reaction. In addition, other lanes were used as marker or references. Therefore, the result of 3.5% agarose gel preliminarily verified the feasibility of EDR and CHA reaction.

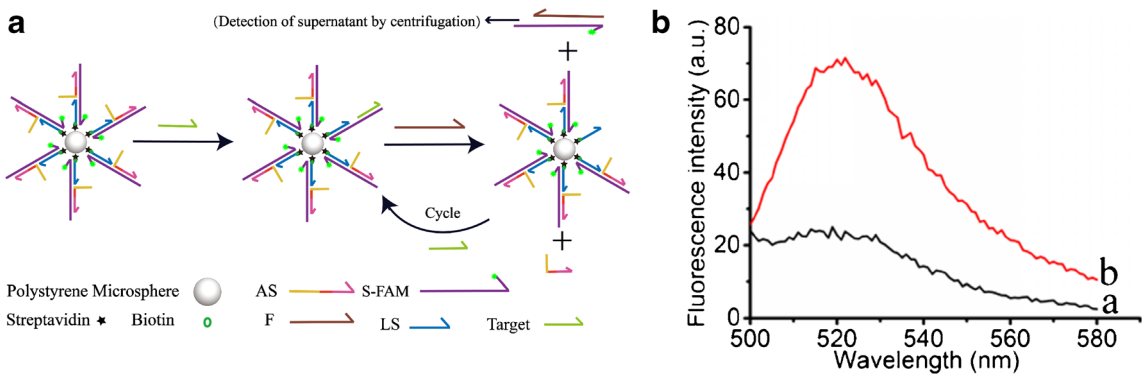

Fig. 1 **a** Schematic illustration of single entropy-driven 3-D DNA walking machine. **b** Verification of entropy-driven 3-D DNA walking machine alone: (*a*) C3 + F, (*b*) C3 + F + T

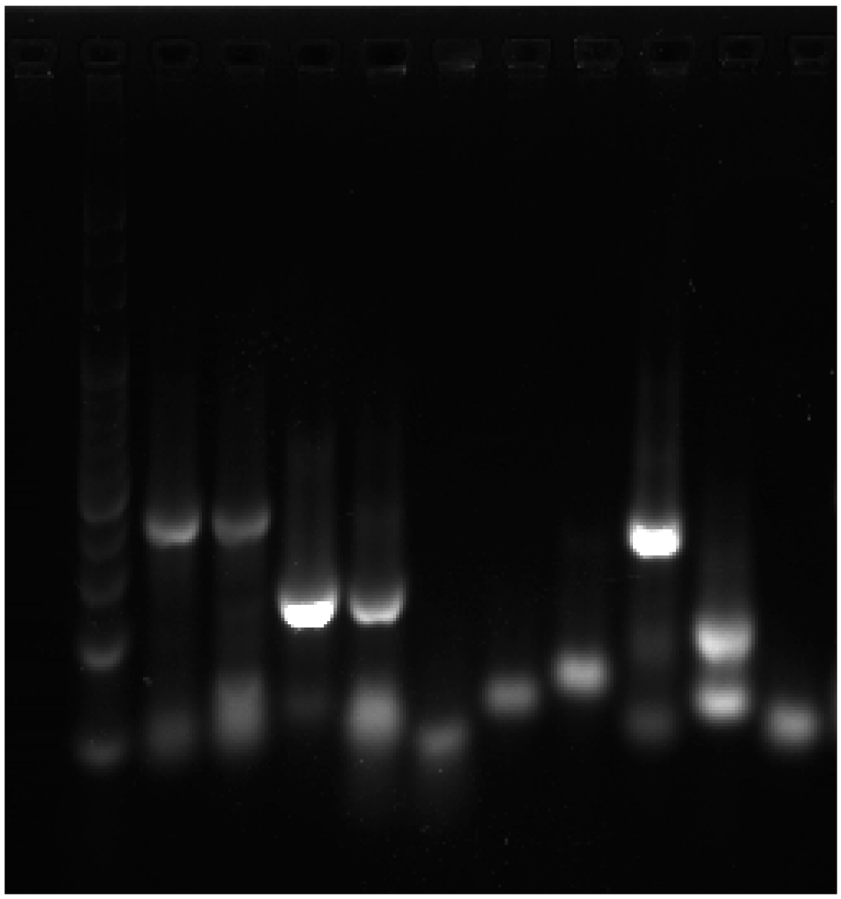

Fig. 2 The 3.5% agarose gel electrophoresis analysis of the biosensor. Different samples were added into lane 1: 20 bp DNA marker, lane 2: 1 μM C3, lane 3: 1 μM (C3 + F), lane 4: 1 μM (F + S), lane 5: 1 μM (C3 + F + microRNA 21), lane 6: 2 μM microRNA 21, lane 7: 2 μM F, lane 8: 2 μM S, lane 9: 1 μM (AS+H1 + H2), lane 10: 1 μM (H1 + H2), lane 11: 2 μM AS

Subsequently, we proved the feasibility of our combined strategy. Figure 3a shows in the absence of entropy-driven 3-D DNA walking machine, the CHA displayed negligible background fluorescence. And then there was a small increased background signal in combining entropy-driven 3-D DNA walking machine and CHA (curve b). In contrast to background signal, in the presence of 10 nM T, the signal increased remarkably (curve c) at 520 nm which means the combination of entropy-driven 3-D DNA walking machine and CHA strategy was feasible. It is noteworthy that the signal-to-noise ratio of entropy-driven 3-D DNA walking machine alone (Fig. 1b) indeed lower than the combined biosensor (Fig. 3a), which has more excellent and efficient signal

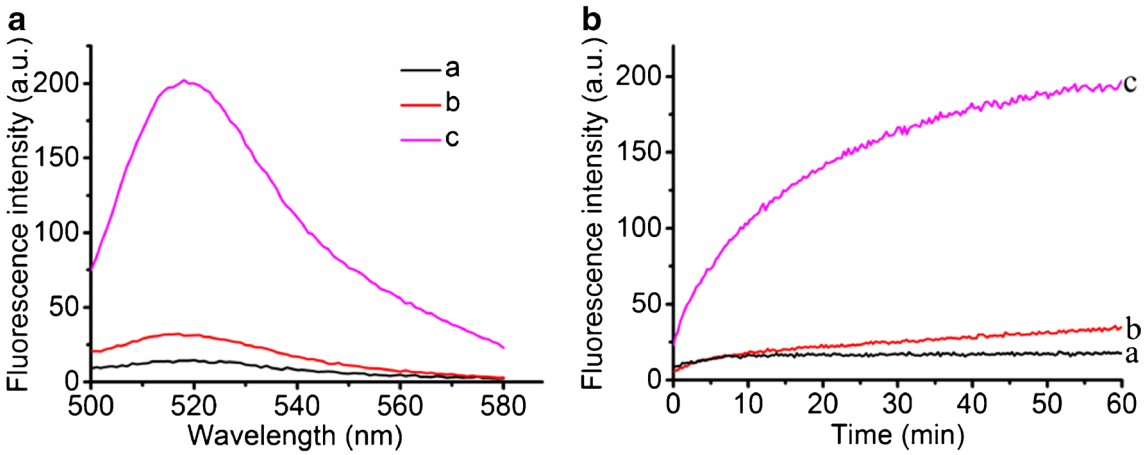

Fig. 3 **a** Feasibility of the combined biosensor: (*a*) CHA in the absence of target; (*b*) entropy-driven 3-D DNA walking machine and CHA in the absence of target; (*c*) entropy-driven 3-D DNA walking machine and CHA in the presence of target. **b** The kinetics of the reaction system: (*a*) CHA in the absence of target; (*b*) entropy-driven 3-D DNA walking machine and CHA in the absence of target; (*c*) entropy-driven 3-D DNA walking machine and CHA in the presence of target

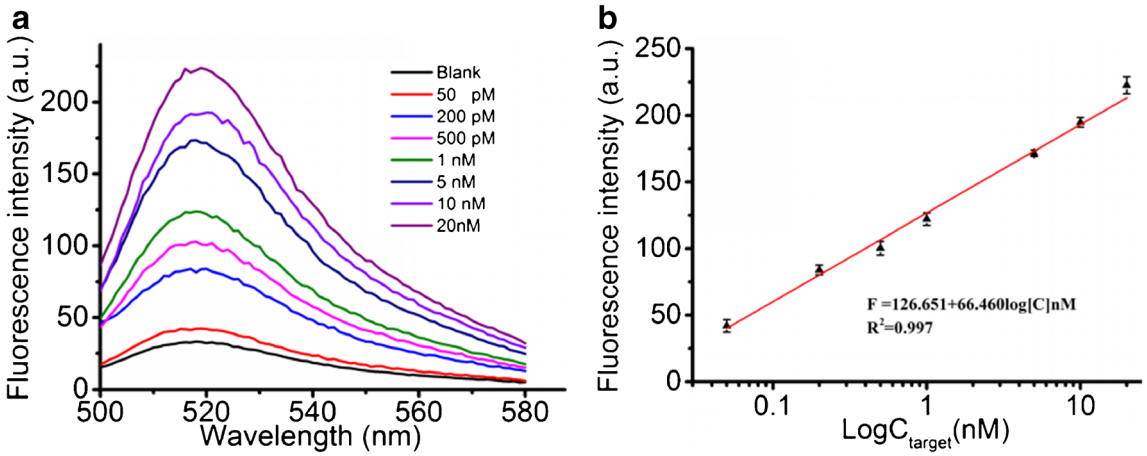

Fig. 4 Analytical performance of the biosensor. Parameters: excitation wavelength, 480 nm; emission wavelength, 520 nm; excitation slit = 5 nm; emission slit = 10 nm. **a** Fluorescence emission spectra in the presence of target at different concentrations (from a-h: 50 pM, 200 pM, 500 pM, 1 nM, 5 nM, 10 nM, 20 nM). **b** linear relationship between the intensity and the logarithm of various target concentrations. Error bars represented standard deviations of the measurements ($n = 3$)

amplification efficiency. The kinetics of the reaction system is illustrated in Fig. 3b.

Analytical performance of the method

To explore the sensitivity of the developed fluorescent biosensor, various concentrations of microRNA were used under the optimum conditions. As shown in Fig. 4a, it is obvious that a gradual enhanced fluorescence signals in the fluorescent peak at 520 nm is observed with an increase in the concentration of microRNA. In addition, the signals vary linearly with logarithm of microRNA concentration in the range from 50 pM to 20 nM (Fig. 4b). The linear regression equation is F = 126. 651 + 66. 460log[C] (nM) (C represents the concentration of microRNA, F denotes the intensity) with a correlation coefficient (R^2) of 0.997. The limit of detection (LOD) is calculated to be 41 pM. Besides, the comparison with other methods is listed in **Table. S2**, which means the strategy was superior to those of some reported methods.

Specificity and reproducibility of the method

As is known to all, specificity is a necessary feature for evaluating the success of the proposed biosensing strategy. Thus, the specificity of the proposed system was investigated in the presence of four homologous kinds of microRNA, including let-7d, microRNA 141, microRNA 15a, microRNA 200b under identical conditions. As shown in Fig. 5, the signal of $\Delta F_{520\ nm}$ is strong in the presence of 10 nM microRNA 21. We defined $\Delta F_{520\ nm} = (F\text{-}F_0)/F_0$, where F is the measured data of fluorescence intensity at 520 nm, F_0 is the control at 520 nm measured without microRNA-21. It is remarkable that

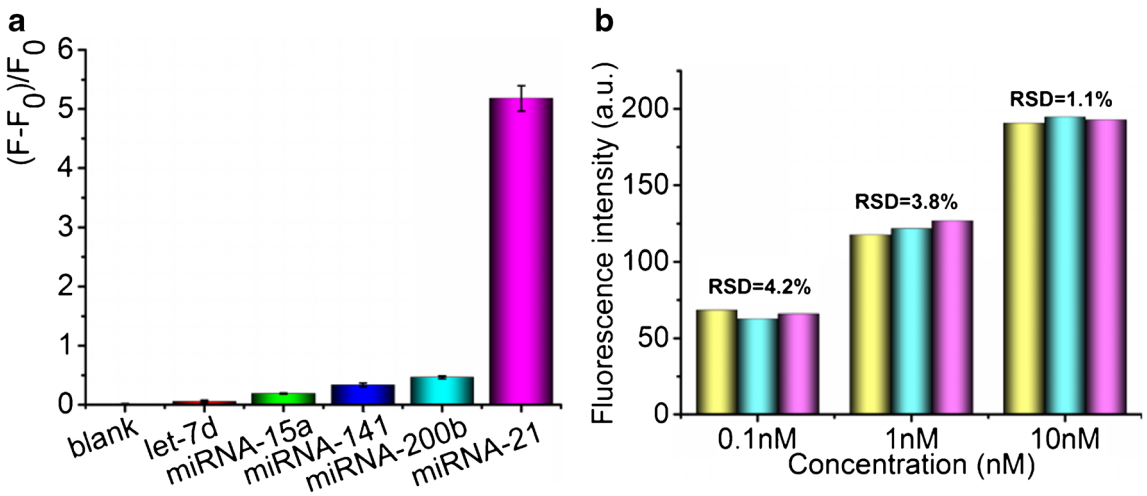

Fig. 5 **a** Specificity investigation of different microRNA. The concentration of microRNA was 10 nM. **b** Reproducibility of the method in different concentration. Error bars represented standard deviations of the measurements ($n = 3$)

Table 1 Analytical recoveries of the proposed assay in detecting microRNA-21 spiked human serum samples

Sample	Add RNA	Found RNA (Mean ± SD)	Recovery (%)
1	200pM	199.6 ± 6.4 pM	99.8
2.	1 nM	1.0 + 0.1 nM	100.0
3	5 nM	5.2 + 0.2 nM	104.0

low signals are observed in contrast to the high fluorescence signals triggered by the target microRNA. The signal of let-7d, microRNA 141, microRNA 15a, microRNA 200b each accounted for 1.1%, 3.7%, 6.5% and 9.0% of the signal of microRNA 121, respectively. Therefore, the method shown superior selectivity and specificity for microRNA detection. In fact, the ability of the biosensor to differentiate homologous microRNA is benefiting from entropy-driven reaction. In this system, the thermodynamics and kinetics of the reaction are firmly coupled, thus the binding free energy (ΔG) of this DNA circuit reach dynamic equilibrium. Even though the change of one base greatly impacts the ΔG and decreases the hybridization efficiency. Reproducibility of the method was further tested by repeating three different concentrations of microRNA21 including 0.1 nM, 1 nM and 10 nM. As is depicted in Fig. 5b, the relative standard deviations (RSD) towards the mentioned-above concentration were 4.2%, 3.8% and 1.1%, respectively. These results suggest that this sensing strategy has satisfactory reproducibility.

Practicability of the microRNA detection platform

To evaluate the practicability of the proposed method in biological samples, the target microRNA-21 was detected using a standard addition to spiked human serum samples. Different target concentrations were added with standard addition method in 10-fold diluted (DEPC H_2O) human serum samples, which are collected from the first affiliated hospital of Chongqing Medical University. As shown in Table. 1 the calculated recovery values were between 99.8% and 104.0%, implying that the strategy represented a satisfactory mean for nucleic acid detection in complex sample.

Conclusions

We designed an entropy-driven 3-D DNA walking machine coupling CHA reaction. The proposed biosensor was successfully used for microRNA-21 detection at picomolar level, which manifested several attractive features. Firstly, it is an enzyme-free system without rigorous reaction conditions and abandons tedious thermal cycling protocol. Furthermore, we use streptavidin-coated polystyrene microspheres as track carrier with promising reproducibility and view target as a stochastic DNA walker with a simple design of structure. Finally, the composite biosensor shows outstanding specificity toward homologous microRNAs and satisfactory performance in reproducibility test (between 1.1% and 4.2%). However, the major limitations of our work include: A. the detection limit of the assay is not low enough compared with those enzyme-based methods; B. Validation of the method in real samples has not been done. An improved strategy of robust enough assay for quantification of serum microRNA in lower abundance will be adapted for the point-of-care clinical diagnosis in our future work.

Acknowledgments This research work was financially supported by the National Natural Science Foundation of China (No. 81672112, 81702101), Chongqing Technology Innovation and Application Demonstration Project (cstc2018jscx-msybX0010) and Key Project of Education Department of Sichuan (No. 16ZA0181).

Compliance with ethical standards The author(s) declare that they have no competing interests.

References

1. Yurke B, Turberfield AJ, Mills AP, Simmel FC, Neumann JL (2000) A DNA-fuelled molecular machine made of DNA. Nature 406(6796):605–608
2. Zhuang JY, Lai WQ, Chen GN, Tang DP (2014) A rolling circle amplification-based DNA machine for microRNA screening coupling catalytic hairpin assembly with DNAzyme formation. Chem Commun 50(22):2935–2938
3. Hwang MT, Wang ZJ, Ping JL, Ban DK, Shiah ZC, Antonschmidt L, Lee J, Liu YS, Karkisaval AG, Johnson ATC, Fan CH, Glinsky G, Lal R (2018) DNA Nanotweezers and graphene transistor enable label-free genotyping. Adv Mater 30(34):1802440
4. Li LD, Li N, Fu SN, Deng YN, Yu CY, Su X (2019) Base excision repair-inspired DNA motor powered by intracellular apurinic/apyrimidinic endonuclease. Nanoscale 11(3):1343–1350
5. Lv SZ, Zhang KY, Zeng YY, Tang DP (2018) Double photosystems-based 'Z-Scheme' Photoelectrochemical sensing mode for ultrasensitive detection of disease biomarker accompanying three-dimensional DNA Walker. Anal Chem 90(11):7086–7093
6. AmicroRNA Y, Ben-Ishay E, Levner D, Ittah S, Abu-Horowitz A, Bachelet I (2014) Universal computing by DNA origami robots in a living animal. Nat Nanotechnol 9(5):353–357
7. Wilner OI, Willner I (2012) Functionalized DNA nanostructures. Chem Rev 112(4):2528–2556
8. Yuan L, Giovanni M, Xie JP, Fan CH, Leong DT (2014) Ultrasensitive IgG quantification using DNA nano-pyramids. Npg Asia Mater 6:e112
9. Hwang MT, Landon PB, Lee J, Choi D, Mo AH, Glinsky G, Lal R (2016) Highly specific SNP detection using 2D graphene electronics and DNA strand displacement. P Natl Acad Sci USA 113(26):7088–7093
10. Liu XQ, Lu CH, Willner I (2014) Switchable reconfiguration of nucleic acid nanostructures by stimuli-responsive DNA machines. Acc Chem Res 47(6):1673–1680

11. Li J, Fan CH, Pei H, Shi JY, Huang Q (2013) Smart drug delivery Nanocarriers with self-assembled DNA nanostructures. Adv Mater 25(32):4386–4396
12. Peng LC, Zhang P, Chai YQ, Yuan R (2017) Bi-directional DNA walking machine and its application in an enzyme-free Electrochemiluminescence biosensor for sensitive detection of MicroRNAs. Anal Chem 89(9):5036–5042
13. Liu MH, Cheng J, Tee SR, Sreelatha S, Loh IY, Wang ZS (2016) Biomimetic autonomous enzymatic Nanowalker of high fuel efficiency. ACS Nano 10(6):5882–5890
14. Wang DF, Vietz C, Schroder T, Acuna G, Lalkens B, Tinnefeld P (2017) A DNA Walker as a fluorescence signal amplifier. Nano Lett 17(9):5368–5374
15. Tomov TE, Tsukanov R, Glick Y, Berger Y, Liber M, Avrahami D, Gerber D, Nir E (2017) DNA bipedal motor achieves a large number of steps due to operation using microfluidics-based Interface. ACS Nano 11(4):4002–4008
16. Zhang P, Jiang J, Yuan R, Zhuo Y, Chai YQ (2018) Highly ordered and field-free 3D DNA nanostructure: the next generation of DNA Nanomachine for rapid single-step sensing. J Am Chem Soc 140(30):9361–9364
17. De Luna P, Mahshid SS, Das J, Luan BQ, Sargent EH, Kelley SO, Zhou RH (2017) High-curvature Nanostructuring enhances probe display for biomolecular detection. Nano Lett 17(2):1289–1295
18. Li W, Wang L, Jiang W (2017) A catalytic assembled enzyme-free three-dimensional DNA walker and its sensing application. Chem Commun 53(40):5527–5530
19. Zeng R, Luo Z, Su L, Zhang L, Tang D, Niessner R, Knopp D (2019) Palindromic molecular Beacon based Z-scheme BiOCl-au-CdS Photoelectrochemical biodetection. Anal Chem 91(3):2447–2454
20. Zeng RJ, Luo ZB, Zhang LJ, Tang DP (2018) Platinum Nanozyme-catalyzed gas generation for pressure-based bioassay using polyaniline nanowires-functionalized graphene oxide framework. Anal Chem 90(20):12299–12306
21. Yang XL, Tang YA, Mason SD, Chen JB, Li F (2016) Enzyme-powered three-dimensional DNA Nanomachine for DNA walking, payload release, and biosensing. ACS Nano 10(2):2324–2330
22. Qu XM, Zhu D, Yao GB, Su S, Chao J, Liu HJ, Zuo XL, Wang LH, Shi JY, Wang LH, Huang W, Pei H, Fan CH (2017) An exonuclease III-powered, on-particle stochastic DNA Walker. Angew Chem Int Ed 56(7):1855–1858
23. Wei W, Wei M, Yin LH, Pu YP, Liu SQ (2018) Improving the fluorometric determination of the cancer biomarker 8-hydroxy-2 '-deoxyguanosine by using a 3D DNA nanomachine. Microchim Acta 185(10):494
24. Yin D, Tao YY, Tang L, Li W, Zhang Z, Li JL, Xie GM (2017) Cascade toehold-mediated strand displacement along with non-enzymatic target recycling amplification for the electrochemical determination of the HIV-1 related gene. Microchim Acta 184(10):3721–3728
25. Liang CP, Ma PQ, Liu H, Guo XG, Yin BC, Ye BC (2017) Rational engineering of a dynamic, entropy-driven DNA Nanomachine for intracellular MicroRNA imaging. Angew Chem Int Ed 56(31):9077–9081
26. Zhang DY, Turberfield AJ, Yurke B, Winfree E (2007) Engineering entropy-driven reactions and networks catalyzed by DNA. Science 318(5853):1121–1125
27. He L, Lu DQ, Liang H, Xie ST, Zhang XB, Liu OL, Yuan Q, Tan WH (2018) mRNA-initiated, three-dimensional DNA amplifier able to function inside living cells. J Am Chem Soc 140(1):258–263
28. Liu BW, Wu P, Huang ZC, Ma LZ, Liu JW (2018) Bromide as a robust Backfiller on gold for precise control of DNA conformation and high stability of spherical nucleic acids. J Am Chem Soc 140(13):4499–4502
29. Li YG, Cu YTH, Luo D (2005) Multiplexed detection of pathogen DNA with DNA-based fluorescence nanobarcodes. Nat Biotechnol 23(7):885–889
30. Peng W, Zhao Q, Chen M, Piao J, Gao W, Gong X, Chang J (2019) An innovative "unlocked mechanism" by a double key avenue for one-pot detection of microRNA-21 and microRNA-141. Theranostics 9(1):279–289
31. He MQ, Wang K, Wang WJ, Yu YL, Wang JH (2017) Smart DNA machine for carcinoembryonic antigen detection by exonuclease III-assisted target recycling and DNA Walker Cascade amplification. Anal Chem 89(17):9292–9298
32. Liu JT, Du P, Zhang J, Shen H, Lei JP (2018) Sensitive detection of intracellular microRNA based on a flowerlike vector with catalytic hairpin assembly. Chem Commun 54(20):2550–2553
33. Zhang Y, Luo SH, Bo ST, Chai ZX, Li B, Liu JM, Zheng L (2018) A novel electrochemical cytosensor for selective and highly sensitive detection of cancer cells using binding-induced dual catalytic hairpin assembly. Biosens Bioelectron 102:568–573
34. Yang WT, Zhou XX, Zhao JM, Xu WJ (2018) A cascade amplification strategy of catalytic hairpin assembly and hybridization chain reaction for the sensitive fluorescent assay of the model protein carcinoembryonic antigen. Microchim Acta 185(2):100
35. Bai SL, Wang T, Zhang Z, Sheng SC, Yu W, Xie GM (2017) A novel colorimetric biosensor for detecting target DNA and human alpha thrombin based on associative toehold activation concatemer induced catalyzed hairpin assembly amplification. Sensor Actuat B-Chem 239:447–454